https://doi.org/10.1016/j.apsusc.2017.02.168

Oxygen-dependent epitaxial growth of Pt(001) thin films on MgO(001) by magnetron sputtering

X.Y. Qiu[1)] *, R. X. Wang[1)], G. Q. Li [1)], T. Zhang[1)], L.T. Li[1)], M. L.Wei[1)], X. S. Meng[1)], H.Ji[2)], Z. Zhang[3)], C.H.Chan[3)], J. Y. Dai[3)]

[1)] *School of Physical Science and Technology, Southwest University, Chongqing 400715, China*

[2)]*School of Energy Science and Engineering , University of Electronic Science and Technology of China, Chengdu 610054,Sichuan, China*

[3)] *Department of Applied Physics, the Hong Kong Polytechnic University, Hong Kong, China*

** Corresponding author: Tel.:+86 23-68252355 E-mail address:qxy2001@swu.edu.cn*

Abstract: The roles of oxygen gas in crystal orientation, surface morphology and electrical resistivity of Pt thin films grown on MgO(001) substrate by magnetron sputtering are studied. With a well-controlled oxygen ratio (15% oxygen) during sputtering deposition with Ar-O_2 mixture ambient, (001) epitaxial growth of Pt film on MgO substrate is achieved with an epitaxial orientation relationship of (001)Pt//(001)MgO and [100]Pt//[100]MgO. Microstructural and electrical characterizations reveal that the (001) Pt thin films possess very smooth surface and good conductivity. The formation and subsequent decomposition of platinum oxides in the Pt films grown with more than 30 % oxygen result in an increase of surface roughness and electrical resistivity. The high-quality Pt(001) film has large potential for integrated electronic device applications.

Key words: Pt film, epitaxial growth, oxygen ratio, microstructure

1.Introduction

Thin platinum (Pt) film is commonly used as the bottom electrode or seed layer for ferroelectric oxide thin films due to its good chemical and thermal stability. Pt has a face-centered cubic structure with a lattice constant (0.3924 nm) matching most of the perovskite oxides, such as (Sr,Ba)TiO_3(a= 0.3905 nm), Pb(Zr,Ti)O_3 (a~0.40 nm) and (La,Ca)MnO_3(a~0.38 nm). For example, the excellent lattice match between Pt and $SrTiO_3$ has enabled the epitaxial growth of Pt(001) on $SrTiO_3$(001) by pulsed-laser

deposition, atomic layer deposition, and sputtering [1-5]. Under some artificially tailored deposition conditions, even there is a large lattice mismatch (5-10 %), stable epitaxial Pt films can still be grown on MgO[6-9], Al_2O_3[6], buffer layer-covered Si [10-13], SiN[14], Fe_3O_4[15], ZrO_2[16-17] and sapphire[18-19]. Compared to [111]-orientation, it is more difficult to prepare stable Pt thin films with [001]-preferred orientation on the same conditions, because Pt(001) plane has a higher surface energy (1286 erg/cm^2) than Pt(111) plane (977 erg/cm^2) [20]. Therefore, even on the (001) substrate of cubic oxide material, the Pt film still prefers [111] growth orientation because the close-packed growth favors the growth along [111] directions. Moreover, due to its high activation energy of diffusion, the [001]-orientated Pt films need high deposition/annealing temperature (> 500℃), and usually exhibit a cross-hatched surface pattern [3] or pinhole microstructure[14], which greatly suppress the uniformity and density of Pt film. MgO has a higher surface energy (1200 erg/cm^2) than other oxide materials, suggesting that it is highly desirable for the c-oriented Pt film growth. In our previous work [21], oxygen in the sputtering ambient plays a key role in achieving the epitaxial Pt films on MgO(001) substrates. In this paper, we investigate effects of oxygen ratio in sputtering ambient on the crystal structure, surface morphology, and electrical resistivity of Pt films. Under optimized conditions, we have achieved high-quality epitaxial Pt(001) films on MgO(001) with smooth surface and good conductivity.

2. Experimental section

A Pt metal plate with a purity of 99.99 % was used as the sputtering target for depositing thin Pt films on MgO(001) single-crystal substrates. Because MgO has a high chemical activity with water and carbon dioxide in air, there is usually one hydrate or carbonate layer covered on it. Thus, prior to deposition, the re-polishing and pre-heating treatments proposed by M. Huth *et al.* [22-23] are carried out:

First, the MgO(001) single-crystal substrates were re-polished by using an OP-S suspension consisting of 25% SiO_2 and 75% H_2O for 4h. Then, the substrates were cleaned in ethanol, dried by pure nitrogen, put in the chamber with a basic pressure of 2.4×10^{-4} Pa, and finally pre-heated at 700℃ for 1h to obtain a well-ordered surface suitable for epitaxial film growth. About 150 nm-thick Pt films were deposited on treated MgO substrate at 700℃ in 2.7 Pa Ar-O_2 mixed ambient with different oxygen ratios (0, 15, 30 and 45 %) by using dc-sputtering with a working power of 35 W (growth rate is 9±1 nm/min). After deposition, the Pt films were *in-situ* annealed in deposition ambient or pure Ar ambient for 30 min.

Preferred crystal orientations of the grown Pt films were examined by θ-2θ x-ray diffraction, φ-scan and χ-ω map by means of the x-ray double-crystal four-circle diffractometer (XRD, Bede D1). Micro-structural characteristics were performed using transmission electron microscope (TEM, JEM-2100F). The surface morphology was investigated by scanning electron microscope (SEM, JSM-7100F) and atomic force microscope (AFM，Hitachi E-sweep). The electrical resistivity was measured using four-point probe combined with Keithley 2400 sourcemeter.

3. Results and discussions

As discussed in the introduction, our previous work [21] has revealed that an oxygen-containing ambient is necessary for the epitaxial growth of [001]-oriented Pt films on MgO substrates. Therefore, we firstly investigated effects of the oxygen ratio in Ar-O_2 mixed ambient on the microstructures of the Pt films on MgO(001) substrates. Fig.1 shows θ-2θ XRD patters for the Pt films on MgO(001) substrates deposited in 2.7 Pa Ar-O_2 mixed ambient with different oxygen ratios (0, 15, 30, 45 %). Because the signal from MgO single-crystal substrates is too strong, all the XRD patterns are plotted using a logarithm-type Y-axis. As shown in Fig.1, the Pt film deposited in pure Ar ambient (0 % oxygen) is

polycrystalline exhibiting three peaks: Pt(111), Pt(002) and Pt(220). When the oxygen ratio in sputtering ambient reaches 15 %, Pt(220) peak vanishes and Pt(111) peak becomes very weak; while Pt (002) peak becomes as strong as MgO(002) peak. After *in-situ* annealing the film at 700°C in 15 % oxygen ambient for 30 min, the Pt(111) peak becomes obvious again; while annealed in pure Ar ambient for 30 min, the Pt(111) peak vanishes, only a strong Pt (002) peak retains (as shown in Fig.2), revealing the epitaxial growth of Pt(001) film on MgO. However, it is noted that the Pt(002) peak gradually decreases with further increase of oxygen ratio, and when the oxygen ratio reaches 30 %, one weak peak belongs to Pt_3O_4(320) can be seen. When the oxygen ratio reaches 45 %, the Pt_3O_4(320) peak becomes much stronger than the Pt(002) peak; Moreover, the once vanished Pt (111) and Pt (220) peaks appear again. This result reveals that the Pt films are oxidized and poly-crystallized again when the oxygen ratio is higher than 30 %. In order to investigate the crystallinity of the [001]-oriented Pt films deposited with 15 and 30 % oxygen, their rocking curves taken at Pt (002) diffraction were also measured. As shown in Fig.3, for the Pt film deposited with 15 %-oxygen, the full width at half maximum (FWHM) of Pt (002) reflection is 0.17°, which is smaller than that (0.23°) of the Pt film deposited with 30 % oxygen, showing higher [001]-oriented epitaxial quality. Based on above XRD investigation results, the optimized oxygen ratio for growing epitaxial Pt (001) film on MgO (001) is determined to be 15 %.

Figure 4 shows SEM images of Pt films deposited with different oxygen ratios. As seen from Fig.4a, the film deposited in pure Ar (0 % O_2) is polycrystalline with an average particle size of 20-30 nm. For the film deposited with 15 % oxygen, it exhibits a smooth surface composed by rectangular terraces (Fig.4b), which is the typical surface morphology for the Pt (001) plane. While for the film grown with 30 % oxygen, those rectangular terraces become more distinguishable, but some square pores appear, as

shown as Fig.4c. It can be also see in Fig.4d that when the oxygen ratio increases to 45 %, the Pt film exhibits percolating Pt networks infiltrated with interconnected nano-sized pores, resulting in an increased surface roughness and pores. This phenomenon is similar to what has been reported by Jung *et al.*[24]: these pores come from the formation and decomposition of platinum oxides with accompanied loss of oxygen during the 700℃-deposition process.

Table 1 Resistivity of Pt films deposited in Ar-O_2 mixed ambient with different oxygen ratios

Sputtering ambient	Resistivity (Ω·m)
100 % Ar (0 % oxygen)	2.94×10^{-7}
85 % Ar +15 % O_2	1.51×10^{-8}
70 % Ar + 30 % O_2	1.70×10^{-8}
55 % Ar + 45 % O_2	2.72×10^{-7}

Table 1 lists the electrical resistivity of Pt films deposited with different oxygen ratios. The Pt film grown with 15 % oxygen exhibits the smallest resistivity of $1.51\times10^{-8}\Omega$.m, while the Pt film grown with 45% oxygen shows a resistivity as high as $2.72\times10^{-7}\Omega \cdot$ m. The possible reason for the decrease of conductivity of Pt film with an increased oxygen ratio is the formation of platinum oxides. However, one may also notice that the Pt film grown in pure Ar ambient (0 % oxygen) possesses higher resistivity ($2.94\times10^{-7}\Omega$.m) than that of the Pt film grown with 15% oxygen. This resistivity difference can be attributed to their deference on the film crystallinity and morphology: the Pt film grown in pure Ar ambient (0 % oxygen) is polycrystalline with a loose and rough surface, while the Pt (100) film grown with 15% oxygen exhibits a dense and smooth surface as revealed by SEM investigations (see Fig.4). Above SEM and electrical resistivity investigation results demonstrate again that the Ar-O_2 ambient with

15% oxygen is the optimized ambient for growing epitaxial Pt films on MgO (001) substrates. How to understand the fact that a small amount of oxygen (15 %) improves the epitaxial growth of Pt(100) film on MgO(100) substrate? There are two possible reasons: (1) Like what the hydrogen does to flatten the $SrTiO_3$ surface energy level [25], oxygen atoms reduce oxygen vacancies formed at high temperature (700℃) on the surface of MgO substrates and decrease the surface barrier of MgO, thus improve the epitaxial growth of [001]-oriented Pt. (2) The other reason is sulfur impurities in the Pt target, since sulfur is usually used as a catalyst to purify Pt in metallurgical manufactures. Because the concentration of sulfur-containing impurities is less than 0.0002% (data come from the supplier of Pt target (MTI Corp.)) , we failed to detect it by energy-dispersive x-ray spectrum and x-ray photoelectron spectrum, but Tsong *et al.*[26] have observed the segregation of sulfur on the metal surface at high temperature even though the bulk impurity content is less than 100 ppm. Moreover, Chen *et al.*[2] have systematically discussed the existence possibility of sulfur-containing impurities in the Pt target and effects of oxygen on the epitaxial growth of Pt film on $SrTiO_3$(100) substrates. We believe that similar phenomena also appeared in our experiments, i.e., sulfur-containing impurities deposited on MgO surface act as nucleation seeds for the Pt (111) close-packed growth based on the 3-D island growth mode[16]. Fortunately, the introduced oxygen atoms react with sulfur atoms to form volatile sulfur oxides at high temperature, which can be pumped out from the chamber during the deposition/annealing progress. Therefore, a highly epitaxial [001]-oriented Pt can be achieved. But it should be pointed out that if the oxygen ratio exceeds a certain level, excess oxygen atoms should result in the oxidation of Pt. During the subsequent high-temperature (> 600℃) depositing/annealing progress, the decomposition of platinum oxides should result in the appearance of nanopores on the surface of Pt film (see Fig.4c and 4d)

Effects of annealing ambient on the morphology of Pt films deposited with 15 % oxygen were also investigated. For the flat surface of the as-deposited sample (Fig.5a), annealing treatments make it more rough and non-uniform: more cliffy terraces and square pinholes are observed for the sample annealed in 15 % oxygen ambient (Fig.5b), while some " hillocks " emerge on the surface of the sample annealed in pure argon(Fig.5c). The possible reason is that, when annealing the as-deposited Pt film in oxygen-rich ambient, oxygen atoms not only oxidize sulfur atoms to volatile sulfur oxides, but also oxidize platinum atoms to platinum oxides. The former one can be pumped out the chamber during depositing process, while the later one will decompose during the subsequent 700℃-annealing process, thus results in the appearance of cliffy terraces and square pinholes. Similar result has been observed by W. C. Jung *et al.* [24]. On the other hand, the oxygen-enhanced self-diffusion and agglomeration of metal atoms at the high temperature also contribute to the growth of pinholes[27-30]. By contrast, after annealing the sample in pure argon ambient at high temperature, the surface reconstruction on the basis of the thermal stress relaxation [14] or elastic interaction between the film and the substrate [29] acting as a driving force for the formation of "hillock" on the argon-annealed sample surface.

In order to characterize the surface roughness of as-deposited Pt films grown with 15 % oxygen, atomic force microscopy investigation was also employed. As shown in Fig.6a, the surface is full of steps /terraces and some "pores", but the surface roughness is only about 3.31nm in a 4×4 μm^2 area, and the root mean square roughness (R_{rms}) is only 0.47 nm. These steps are faceted with fixed direction, suggesting that the Pt film is highly oriented. The corresponding line profile (Fig.6b) shows that the smallest step height is about 0.9 nm, and the largest "pores" depth is about 2.7 nm, all of them are very close to multiples of a unit cell height (0.4 nm) of the cubic Pt structure. Moreover, it is noticed that those

steps have sharp cliff, implying that the Pt film favors the growth in cube-on-cube mode rather than the layer-by-layer mode which the film should be grown with half unit cell height.

The in-plane orientations for Pt(111) thin film on MgO (001) single-crystal substrates were investigated by using the x-ray double-crystal four-circle diffractometer. The ϕ - scans of the cubic Pt{111} and cubic MgO{111} reflections are shown in Fig.7a. We can see that both of them show very nice four-fold symmetry diffraction peaks with an interval of 90° from 0 to 360°. This reveals that thin Pt films have significant growth characteristic of in-plane orientation, as we expected. The x-ray χ-ω map of Pt{111} has been measured by the symmetrical diffraction geometry (here the in-plane Bragg angle set-up is $\omega = 19.85^{\circ}$, $2\theta = 39.79^{\circ}$ and $\chi = 47.56^{\circ}$), where a strong dispersion of Pt {111} poles is observed (Fig.7b). Pt{111} reflections on the χ-ω map display four symmetrical spots with 90° distinction. Moreover, the intensity of four poles on Pt{111} reflections is evenly distributed. The ϕ - scans and χ-ω map analyses reveal that the Pt film grown on MgO(001) substrate is highly oriented along the [00h] direction and exhibits a good in-plane relationship of (100)Pt// (100) MgO and (010)Pt//(010)MgO.

Fig. 8a is a cross-section HRTEM image of the Pt/MgO interface observed along the [100] zone axis. There are no voids at the Pt/MgO interface, indicating good adhesion at atomic level. However, a interfacial mismatch-induced dislocation network (pointed by arrows in inset) can be observed at the Pt/MgO interface. These dislocations release the tensile stress from the lattice mismatch between Pt and MgO lattice and facilitate the epitaxial growth of Pt film along [001] direction. Fig.8b shows the corresponding selected-area diffraction pattern (SADP) of the Pt(001)//MgO(001) interface. We can see that Pt diffraction dots almost comply with the 4-fold symmetry of the MgO(001) surface, demonstrating that the Pt/MgO orientation relationship is cube-on-cube. This confirms the results obtained by ϕ -scans

and χ-ω map in the XRD analysis.

4 Conclusions

In conclusion, effects of oxygen gas on morphology, crystal structure and electrical resistivity of Pt films grown on MgO(001) substrates have been investigated. High-quality epitaxial Pt (001) films have been successfully prepared on MgO(001) using magnetron sputtering in a Ar-O_2 mixed ambient with a 15 % oxygen ratio. With the increase of oxygen ratio, the surface roughness of Pt film increases. Moreover, platinum oxides are formed after the oxygen ratio is more than 30 %, resulting in the increase of electrical resistivity of Pt film. The epitaxial growth of Pt on MgO(001) is based on a cube-on-cube model, and the interfacial dislocation network is formed to relax the lattice mismatch-induced strain and facilitate the epitaxial growth of the Pt film. High-quality epitaxial Pt film has large potential to be used as a template for the growth of many functional materials thin films for device applications.

Acknowledgements

This work is supported by the National Natural Science Foundation of China (grant number 11274257), the Natural Science Foundation of Chongqing (grant number cstc2014jcyjA40029) and the Fundamental Research Fund for the Central Universities of China (grant numbers XDJK2014B043,XDJK2016E123).

References

[1] X. Chen, T. Garrent, S. W. Liua, Y. Lina, Q. Y. Zhang, C. Dong, C. L. Chen, Scanning tunneling microscopy studies of growth morphology in highly epitaxial c-axis oriented Pt thin film on (0 0 1) $SrTiO_3$. Surf. Sci. 542(2003) 655–661.

[2] X. M. Xu, J. Liu, Z. Yuan, J. Weaver, C. L. Chen, Y. R. Li, H. J. Gao, N. Shi, Single crystalline highly epitaxial Pt thin films on (0 0 1) $SrTiO_3$. Appl. Phys. Lett. 92(2008) 102102.

[3] J. Son, J. Cagnon, S. Stemmer, Strain relaxation in epitaxial Pt films on (001) $SrTiO_3$. J. Appl. Phys. 106(2009) 043525.

[4] A. Kahsay, M. C. Polo, C. Ferrater, J. Ventura, J. M. Rebled, M. Varela, Growth of epitaxial Pt thin films on (0 0 1) $SrTiO_3$ by rf magnetron sputtering. Appl. Surf. Sci. 306 (2014) 23–26.

[5] J. J. Pyeon, J. Y. Kang, S. H. Baek, C. Y. Kang, J. S. Kim, D. S. Jeong, S. K. Kim, Orientation-controlled growth of Pt films on $SrTiO_3$ (001) by atomic layer deposition. Chem. Mater. 27(2015) 6779–6783.

[6] B. M. Lairson, M. R. Visokay, R. Sinclair, S. Hagstrom, B. M. Clemens, Epitaxial Pt(001), Pt(110), and Pt(l11) films on MgO(001), MgO(110), MgO(l11), and $A1_2O_3$(0001). Appt. Phys. Lett. 61(1992) 1390–1392.

[7] J. Narayan, P. Tiwarr' , K. Jagannadham, O. W. Holland, Formation of epitaxial and textured platinum films on ceramics-(100) MgO single crystals by pulsed laser deposition. Appl. Phys. Let. 64(1994) 2093–2095.

[8] C. Gatel, P. Baules, E. Snoeck, Morphology of Pt islands grown on MgO (001). J. Cryst. Growth 252(2003) 424–432.

[9] T. Matsumoto, K. Tamai, Y. Murashima1, K. Komaki1, S. Nakagawa, Development of Pt/MgO(100) buffer layers for orientation control of perovskite oxide thin films. Jpn. J. Appl. Phys. 47(2008) 7565–7569.

[10] P. Tiwari, X. D. Wu, S. R. Foltyn, Q. X. Jia, I. H. Campbell, P. A. Arendt, R. E. Muenchausen, D. E. Peterson, T. E. Mitchell, J. Narayan, Synthesis of epitaxial Pt on (100)Si using TiN buffer layer by pulsed laser deposition. Appl. Phys. Lett. 65(1994) 2693–2695.

[11] D. Akai, K. Hirabayashi, M. Yokawa, K. Sawada, M. Ishida, Epitaxial growth of Pt (001) thin films

on Si substrates using an epitaxial γ-Al_2O_3(0 0 1) buffer layer. J. Cryst. Growth 264 (2004) 463–467.

[12] S. Gsell, M. Fischer, M. Schreck, B. Stritzker, Epitaxial films of metals from the platinum group (Ir, Rh, Pt and Ru) on YSZ-buffered Si(111). J. Cryst. Growth 311(2009) 3731–3736.

[13] D. Ferrah, M. ElKazzi, G. Niu, C. Botella, J. Penuelas, Y. Robach, L. Louahadj, R. Bachelet, L. Largeau, G. Saint-Girons, Q. Liu, B. Vilquin, G. Grenet, X-ray photoelectron spectroscopy and diffraction investigation of a metal–oxide-semiconductor heterostructure: Pt/Gd_2O_3/Si(111). J. Cryst. Growth 416(2015) 118–125.

[14] S. L. Firebaugh, K. F. Jensen, M. A. Schmidt, Investigation of high-temperature degradation of platinum thin films with an in situ resistance measurement apparatus. J. Microelectromech. S. 7(1998) 128–135.

[15] C. Gatel , E. Snoeck, Epitaxial growth of Au and Pt on Fe_3O_4(111) surface, Surf. Sci. 601(2007) 1031–1039.

[16] H. Galinski, T. Ryll, P. Reibisch, L. Schlagenhauf, I. Schenker, L. J. Gauckler, Temperature-dependent 2-D to 3-D growth transition of ultra-thin Pt films deposited by PLD. Acta Mater. 61(2013) 3297–3303.

[17] H. Galinski, T. Ryll, P. Elser, J. L. M. Rupp, A. Bieberle-Hütter, L. J. Gauckler, Agglomeration of Pt thin films on dielectric substrates. Phys. Rev. B 82(2010) 235415.

[18] R. F. C. Farrow, G. R. Harp, R. F. Marks, T. A. Rabedeau, M. F. Toney, D. Weller, S. S. P. Parkin, Epitaxial growth of Pt on basal-plane sapphire: a seed film for artificially layered magnetic metal structures. J. Cryst. Growth. 133(1993) 47–58.

[19] S. Ramanathan, B. M. Clemens , P. C. McIntyre, U. Dahmen, Microstructural study of epitaxial platinum and permalloy/platinum films grown on (0001) sapphire. Philos. Mag. A 81(2002) 2073–2094.

[20] T. K. Galeev, N. N. Bulgakov, G. A. Savelieva, N. M. Popova, Surface properties of platinum and palladium. React. Kinet. Catal. Lett. 14(1980) 61–65.

[21] Y. Y. Zhang, H. X. Zhu, H. Ji, R. X. Wang, T. Zhang, L.T. Lu. X.Y. Qiu, Microstructures of epitaxial Pt films on MgO and α-Al_2O_3 single-crystal substrates deposited by magnetron sputtering. Chin. Sci. Bull. 61(2016) 1008–1015.

[22] P. Haibach, J. K ö ble, M. Huth, H. Adrian, MgO surface microstructure and crystalline coherence of Co/Pt superlattices. Thin Solid Films 336(1998)168–171.

[23] M. Hutha, C. P. Flynn, Titanium thin film growth on small and large misfit substrates. Appl. Phys. Lett. 71(1997) 2466–2468.

[24] W. C. Jung, J. J. Kim, H. L. Tuller, Investigation of nanoporous platinum thin films fabricated by reactive sputtering: Application as micro-SOFC electrode. J. Power Sources 275(2015) 860–865.

[25] M. S. Wrighton, A. B. Ellis, P. T. Wolczanski, D. L. Morse, H. B. Abrahamson, D. S. Ginley, Strontium titanate photoelectrodes, efficient photoassisted electrolysis of water at zero applied potential. J. Am. Chem. Soc. 98(1976) 2774–2779.

[26] M. Ahmad, T. T. Tsong, Compositional variations in the near surface layers, an atom-probe study of cosegregation of sulfur in Pt–Rh and Pt–Ir alloys. J. Chem. Phys. 83(1985) 388–396.

[27] D. J. Srolovitz, M. G. Goldiner, The thermodynamics and kinetics of film agglomeration. J. Miner Metals Mater. Soc. 47 (1995) 31–36.

[28] E. Jiran, C. V. Thompson, Capillary instabilities in thin films. J. Electr. Mat.19(1990) 1153–1160.

[29] S. K. Sharma, J. Spitz, Hillock formation, hole growth and agglomeration in thin silver films. Thin Solid Films 65(1980) 339–350.

[30] S. P. Murarka, E. Kinsbron, D. B. Fraser, J. M. Andrews, E. J. Lloyd, High temperature stability of PtSi formed by reaction of metal with silicon or by cosputtering. J. Appl. Phys. 54(1983) 6943–6951.

Figure Captions

Figure 1 θ-2θ XRD patterns for the Pt films on MgO(001) substrates deposited in 2.7 Pa Ar-O_2 mixed ambient with an oxygen ratio of 0, 15,30,45 %, respectively.

Figure 2 θ-2θ XRD patterns for (a) the as-deposited Pt films with 15 % oxygen before and after *in-situ* annealing at 700℃ for 30 min in (b) 15 % oxygen and (c) pure Ar ambient, respectively.

Figure 3 Rocking curve of Pt (002) diffraction for the Pt film deposited with (a)15 and (b) 30 % oxygen, respectively.

Figure 4 SEM images for Pt films on MgO(001) substrates deposited in 2.7 Pa Ar-O_2 mixed ambient with an oxygen ratio of (a) 0, (b)15, (c) 30 and (d) 45 %, respectively.

Figure 5 SEM images for (a) as-deposited Pt films with 15 % oxygen before and after *in-situ* annealing at 700℃ for 30 min in (b) 15 % oxygen and (c) pure Ar ambient, respectively.

Figure 6 (a) Atomic force microscopy image and (b) the line profile for the Pt film grown with 15 % oxygen.

Figure 7 (a) X-ray ϕ -scans and (b) χ-ω map for the epitaxial Pt film on MgO(001) taken at {111} reflections of Pt and MgO

Figure 8 (a) The cross-section HRTEM image and (b) corresponding selected area diffraction pattern (SADP) of the Pt(001)//MgO(001) interface for the sample grown with 15 % oxygen. Inset in Fig.8a is the inverse Fourier transform (IFTF) image for the selected area marked with dashed box.

Fig.1

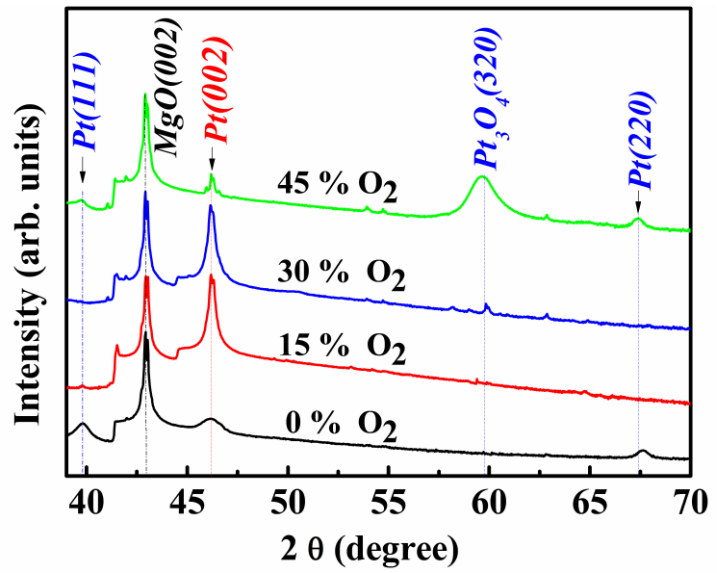

Figure 1 *θ-2θ* XRD patterns for the Pt films on MgO(001) substrates deposited in 2.7 Pa Ar-O_2 mixed ambient with an oxygen ratio of 0, 15,30,45 %, respectively.

Fig.2

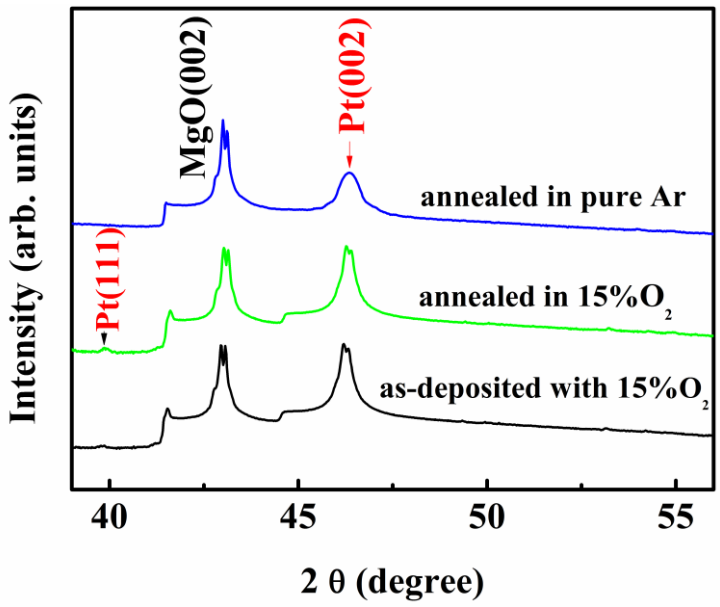

Figure 2 *θ-2θ* XRD patterns for (a) the as-deposited Pt films with 15 % oxygen before and after *in-situ* annealing at 700℃ for 30 min in (b) 15 % oxygen and (c) pure Ar ambient, respectively.

Fig.3

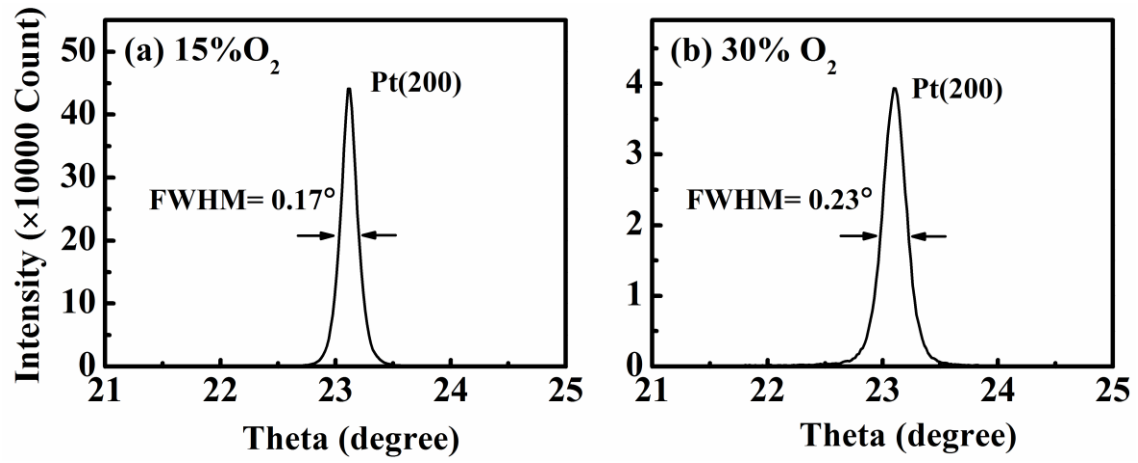

Figure 3 Rocking curve of Pt (002) diffraction for the Pt film deposited with (a)15 and (b) 30 % oxygen, respectively.

Fig.4

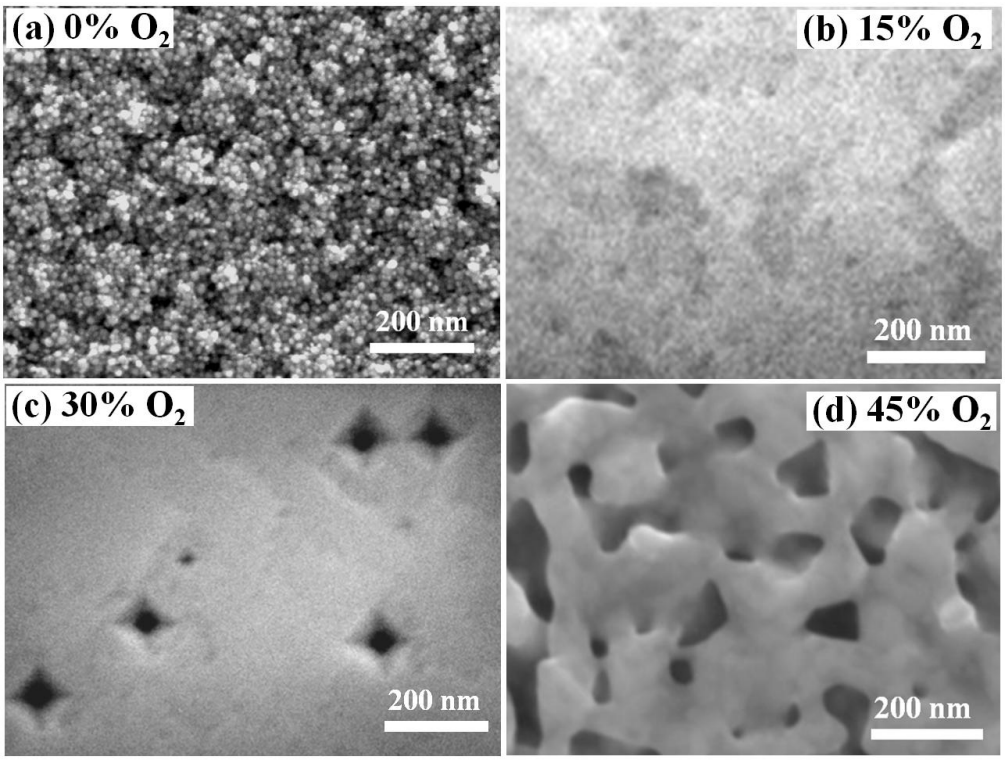

Figure 4 SEM images for Pt films on MgO(001) substrates deposited in 2.7 Pa Ar-O_2 mixed ambient with an oxygen ratio of (a) 0, (b) 15, (c) 30 and (d) 45 %, respectively.

Fig.5

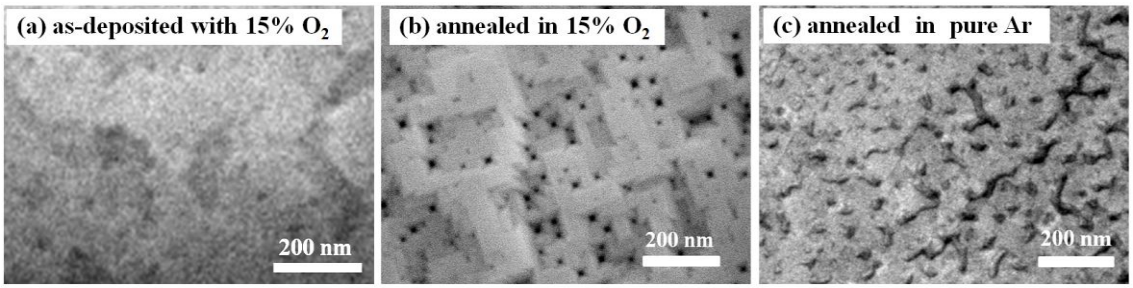

Figure 5 SEM images for (a) as-deposited Pt films with 15 % oxygen before and after *in-situ* annealing at 700℃ for 30 min in (b) 15 % oxygen and (c) pure Ar ambient, respectively.

Fig.6

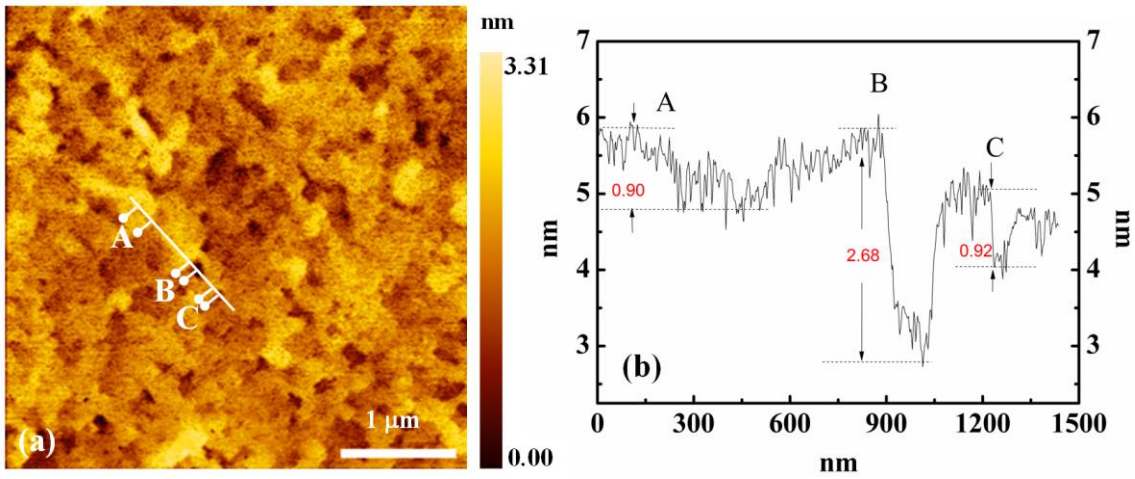

Figure 6 (a) Atomic force microscopy image and (b) the line profile for the Pt film grown with 15 % oxygen.

Fig.7

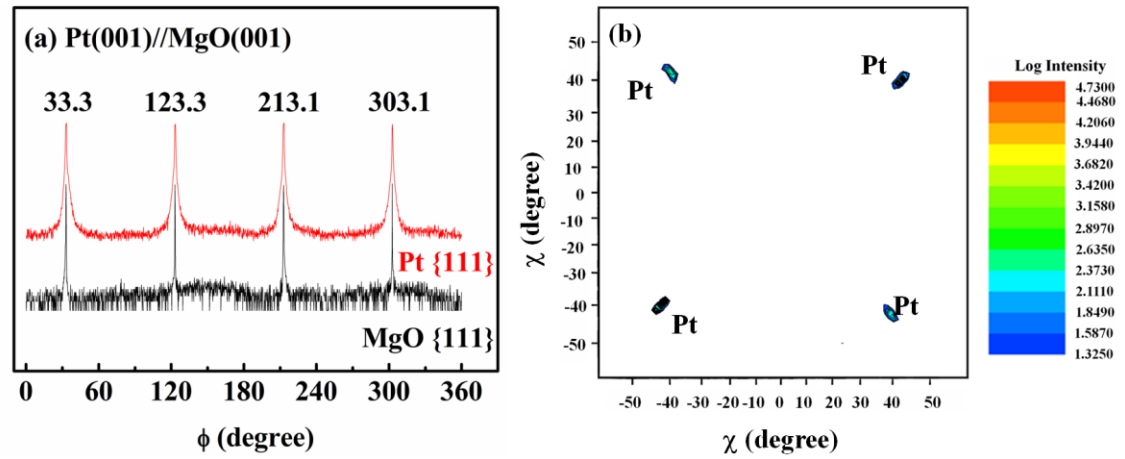

Figure 7 (a) X-ray ϕ -scans and (b) χ-ω map for the epitaxial Pt film on MgO(001) taken at {111} reflections of Pt and MgO

Fig.8

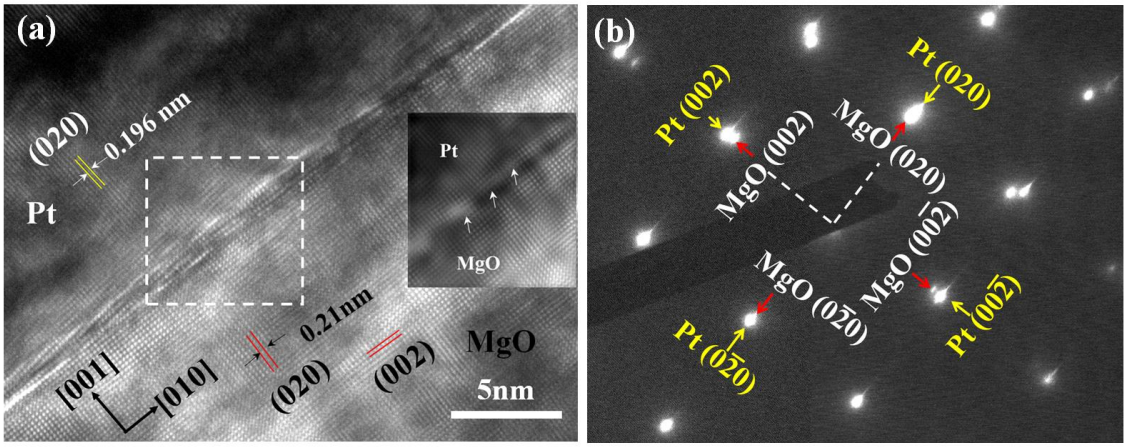

Figure 8 (a) The cross-section HRTEM image and (b) corresponding selected area diffraction pattern (SADP) of the Pt(001)//MgO(001) interface for the sample grown with 15 % oxygen. Inset in Fig.8a is the inverse Fourier transform (IFTF) image for the selected area marked with dashed box.